on the ROI location. Among the scatter correction methods used in this study, the one based on factor analysis gave the best overall results. However, using I10 or JA images also provided a definite improvement compared to I20 images for both qualitative and quantitative image analyses. Clinical studies will now be needed to confirm that scatter correction might play a significant role in scintimammography.

ACKNOWLEDGMENTS

We are grateful to Robert Di Paola, Marie-Gabrielle Dondon, André Gavoille, Nadine Guilabert, Philippe Maksud and Mélanie Pélégrini for their contributions to this work. We also thank the reviewers for their helpful suggestions.

REFERENCES

1. Khalkhali I, Cutrone J, Mena I, et al. Technetium-99m-sestamibi scintimammography of breast lesions: clinical and pathological follow-up. *J Nucl Med* 1995;36:1784–1789.
2. Khalkhali I, Cutrone JA, Mena IG, et al. Scintimammography: the complementary role of Tc-99m sestamibi prone breast imaging for the diagnosis of breast carcinoma. *Radiology* 1995;196:421–426.
3. Taillefer R, Robidoux A, Lambert R, Turpin S, Laperrière J. Technetium-99m-sestamibi prone scintimammography to detect primary breast cancer and axillary lymph node involvement. *J Nucl Med* 1995;36:1758–1765.
4. Villanueva-Meyer J, Leonard MH, Briscoe E, et al. Mammoscintigraphy with technetium-99m-sestamibi in suspected breast cancer. *J Nucl Med* 1996;37:926–930.
5. Tiling R, Sommer H, Pechmann M, et al. Comparison of technetium-99m-sestamibi scintimammography with contrast-enhanced MRI for diagnosis of breast lesions. *J Nucl Med* 1997;38:58–62.
6. Waxman AD. The role of ^{99m}Tc methoxyisobutylisonitrile in imaging breast cancer. *Semin Nucl Med* 1997;27:40–54.
7. Palmedo H, Grünwald F, Bender H, et al. Scintimammography with technetium-99m methoxyisobutylisonitrile: comparison with mammography and magnetic resonance imaging. *Eur J Nucl Med* 1996;23:940–946.
8. Palmedo H, Schomburg A, Grünwald F, Mallmann P, Krebs D, Biersack HJ. Scintimammography with Tc-99m MIBI in suspicious breast lesions. *J Nucl Med* 1996;37:626–630.
9. Buvat I, Benali H, Todd-Pokropek A, Di Paola R. Scatter correction in scintigraphy: the state of the art. *Eur J Nucl Med* 1994;21:675–694.
10. Collier BD, Palmer DW, Knobel J, Isitman AT, Hellman RS, Zielonka JS. Gamma camera energy for Tc^{99m} bone scintigraphy: effect of asymmetry on contrast resolution. *Radiology* 1984;151:495–497.
11. Yanch JC, Irvine AT, Webb S, Flower MA. Deconvolution of emission tomographic data: A clinical evaluation. *Br J Radiol* 1988;61:221–225.
12. Floyd JL, Mann RB, Shaw A. Changes in quantitative SPECT thallium-201 results associated with the use of energy-weighted acquisition. *J Nucl Med* 1991;32:805–807.
13. Rao MG. Bone imaging with energy-weighted acquisition. *J Nucl Med* 1993;34:997–999.
14. Bonnin F, Buvat I, Benali H, Di Paola R. A comparative clinical study of scatter correction methods for scintigraphic images. *Eur J Nucl Med* 1994;21:388–393.
15. Staff RT, Gemmell HG, Sharp PF. Assessment of energy-weighted acquisition in SPECT using ROC analysis. *J Nucl Med* 1995;36:2352–2355.
16. O'Connor MK, Caiati C, Christian TF, Gibbond RJ. Effects of scatter correction on the measurement of infarct size from SPECT cardiac phantom studies. *J Nucl Med* 1995;36:2080–2086.
17. Jaszczak RJ, Floyd CE, Coleman RE. Scatter compensation techniques for SPECT. *IEEE Trans Nucl Sci* 1985;32:786–793.
18. Buvat I, Benali H, Frouin F, Bazin JP, Di Paola R. Target apex-seeking in factor analysis of medical image sequences. *Phys Med Biol* 1993;38:123–138.
19. Buvat I, Rodriguez-Villafuerte M, Todd-Pokropek A, Benali H, Di Paola R. Comparative assessment of nine scatter correction methods based on spectral analysis using Monte Carlo simulations. *J Nucl Med* 1995;36:1476–1488.
20. Maurer AH, Caroline DF, Jadali FJ, et al. Limitations of craniocaudal thallium-201 and technetium-99m-sestamibi mammoscintigraphy. *J Nucl Med* 1995;36:1696–1700.
21. Diggles L, Mena I, Khalkhali I. Technical aspects of prone dependent-breast scintimammography. *J Nucl Med Technol* 1994;22:165–170.
22. Scopinaro F, Schillaci O, Mingazzini PL, et al. Technetium-99m sestamibi: an indicator of breast cancer invasiveness. *Eur J Nucl Med* 1994;21:984–987.
23. Burak Z, Argon M, Memis A, et al. Evaluation of palpable breast masses with $99Tc^{m}$-MIBI: a comparative study with mammography and ultrasonography. *Nucl Med Commun* 1994;15:604–612.
24. Maublant J, de Latour M, Mestas D, et al. Technetium-99m-sestamibi uptake in breast tumor and associated lymph nodes. *J Nucl Med* 1996;37:922–925.

Comparison of Iodotyrosines and Methionine Uptake in a Rat Glioma Model

Karl-Josef Langen, Ralf P. Clauss, Marcus Holschbach, Heinz Mühlensiepen, Jürgen C.W. Kiwit, Karl Zilles, Heinz H. Coenen and Hans-W. Müller-Gärtner

Institutes of Medicine and Nuclear Chemistry, Research Center Jülich, Jülich; and Departments of Neurosurgery and Neuroanatomy, Heinrich-Heine-University of Düsseldorf, Düsseldorf, Germany

This study compares brain tumor imaging with 3-[^{123}I]iodo-α-methyl-L-tyrosine (IMT) and 3-[$^{123/125}$I]iodo-O-methyl-α-methyl-L-tyrosine (OMIMT) to that with [methyl-^{3}H]-L-methionine (Met) in a rat glioma model by double-tracer autoradiography. **Methods:** Cells of the glioma clone F-98 were implanted stereotactically into the right basal ganglia of 22 Fischer 344 rats. After 8 days of tumor growth, the animals simultaneously were injected with a mixture of either ^{123}I-IMT and ^{3}H-Met (n = 5), ^{123}I-OMIMT and ^{3}H-Met (n = 8) or ^{123}I-IMT and ^{125}I-OMIMT (n = 9). The animals were killed 15 min after the tracer injection and cryosections of the tumor-bearing brain area were exposed to phosphor-imaging plates both immediately and after the decay of ^{123}I. Tumor-to-brain ratios (T/B) and intratumoral distribution of the different tracers and of the cresyl violet staining of the tissue were compared. **Results:** There was a significant correlation of the T/B ratios between all tracers (IMT versus Met: $r = 0.97$, $n = 5$, $p < 0.01$; OMIMT versus Met: $r = 0.94$, $n = 8$, $p < 0.001$; OMIMT versus IMT: $r = 0.95$, $n = 9$, $p < 0.001$). Intratumoral tracer distribution was similar for all tracers and the extent of tumor labeling was identical to that of the histological tumor extent. Mean values of the T/B ratios, however, were lower for IMT (2.81 ± 0.78, $n = 14$, mean ± s.d., $p < 0.01$ compared with Met) and for OMIMT (2.03 ± 0.57, $n = 17$, $p < 0.01$ compared with Met) than for Met (3.86 ± 1.12, $n = 13$). **Conclusion:** This study confirms that tumor imaging with IMT is similar to that of Met but T/B ratios of IMT are lower. OMIMT intratumoral tracer distribution and tumor size are similar to Met and IMT, but the T/B contrast is rather low and makes this amino acid less suitable for clinical application.

Key Words: amino acids; 3-[^{123}I]iodo-α-methyl-L-tyrosine; 3-[$^{123/125}$I]iodo-O-methyl-α-methyl-L-tyrosine; [methyl-^{3}H]-L-methionine; cerebral glioma; autoradiography

J Nucl Med 1998; 39:1596–1599

Radiolabeled amino acids such as [methyl-^{11}C]-L-methionine (Met) and PET enlarge the potential of conventional radiological methods for diagnosing cerebral gliomas (*1,2*). One advantage of using amino acids appears to be visualization of the degree of intracerebral infiltration by gliomas (*3,4*). In recent years, the synthetic amino acid L-3-[^{123}I]iodo-α-methyltyrosine (IMT) has been used for brain tumor imaging, which can be used in SPECT (*5–7*).

IMT is transported into the brain and into brain tumors like other large neutral amino acids (*6,8*), and its uptake can be

Received Sep. 2, 1997; revision accepted Dec. 19, 1997.

For correspondence or reprints contact: Karl-Josef Langen, MD, Institute of Medicine, Research Center Jülich, P.O. Box 1913, 52425 Jülich, Germany.

inhibited specifically by infusion of L-amino acids (*7*). Although there is no incorporation of IMT into cerebral proteins (*6,8*), this tracer shows a similar diagnostic potential to Met. This is explained by the fact that transport phenomena play an important role for the increased accumulation of amino acids in cerebral gliomas (*9–11*). Initial clinical investigations have indicated the potential of SPECT with IMT for tumor grading, diagnosis of recurrence and therapeutic response (*12–14*).

We previously compared PET with Met and SPECT with IMT in patients with cerebral gliomas (*15*). In that study, the imaging of tumor extent was identical and there was a significant correlation of tumor-to-brain (T/B) ratios of both tracers within 1 hr postinjection. T/B ratios, however, were significantly lower for IMT than for Met. It remained unclear to what extent this difference was due to methodological differences between PET and SPECT or to differences between the tracers. This study compares the T/B ratios of both tracers in a rat glioma model by double-tracer autoradiography. This approach allowed a more accurate comparison of T/B ratios and intratumoral tracer distribution. The autoradiographically detected tumor extent also can be compared with a histological analysis.

A recently introduced analog of IMT, 3-[^{123}I]iodo-O-methyl-α-methyl-L-tyrosine (OMIMT) with higher lipophilicity (*16*) was also included in this study to test its tumor-imaging capacity. This derivative of IMT was developed because brain uptake of IMT is low and a relatively high tracer dose of approximately 500 MBq is needed to obtain optimal brain scans (*15*). This makes this procedure expensive, although the radiation dose is in the range of conventional nuclear medicine investigations (*17*). Experiments in mice have shown that OMIMT shows a five times higher brain uptake than IMT (*16*). It is unknown, however, whether the uptake of this amino acid is increased in brain tumors to the same extent as IMT.

MATERIALS AND METHODS

Radiotracers

Iodine-123-IMT and $^{123/125}$I-OMIMT were prepared as described previously (*16*). Specific radioactivity of IMT was > 170 TBq/mmol (4500 Ci/mmol), the radiochemical yield 80% ± 5% and the radiochemical purity was > 99%. For OMIMT, the specific radioactivity was > 81 TBq/mmol (2200 Ci/mmol), the radiochemical yield 40% ± 5% and the radiochemical purity > 98%. Methyl-^{3}H-Met was obtained commercially (Amersham Buchler, Braunschweig, Germany) with a specific radioactivity of 3.11 TBq/mmol (84 Ci/mmol).

Animal Experiments

Male Fischer 344 rats, 8–12 wk, weight 200–250 g (Charles River Wiga, Sulzfeld, Germany), were kept under standard conditions with free access to food and water. F-98 rat glioma cells (10 μl, 1 × 10^5 cells) were stereotactically implanted (David Kopf Instruments,Tujunga, CA) into the right basal ganglia of the 22 rats while under isofluorane anesthesia. The tumors were allowed to grow for 8 days. Animals were distributed at random into three groups and were reanesthesized for tracer injection. The first group (n = 5) was injected intracardially with a mixture of 22.2 MBq ^{123}I-IMT and 22.2 MBq ^{3}H-Met, the second group (n = 8) with 22.2 MBq ^{123}I-OMIMT and 22.2 MBq ^{3}H-Met and the third group (n = 9) with 22.2 MBq ^{123}I-IMT and 2.2 MBq ^{125}I-OMIMT. Fifteen minutes after tracer injection, the animals were killed, the brains were removed and then quickly frozen in liquid isopentane (−50°C). This time point was chosen because in humans cerebral uptake of IMT reaches a maximum approximately 15 min after injection (*6,15*). For OMIMT, maximal uptake in the brain of mice was observed at 10 min after injection (*16*). The brain was cut into 20-μm sections in a cryostat. The experiments were approved by the district government (Cologne/Germany No. 23.203.2 KFA 6/93).

Autoradiography

Coronal sections of the tumor-bearing brain were exposed to imaging plates (Fuji Photofilm, Tokyo, Japan). In the case of the double-tracer comparison, ^{123}I-IMT versus ^{3}H-Met or ^{123}I-OMIMT versus ^{3}H-Met, respectively, the brain slices were first exposed to ^{3}H-sensitive imaging plates that were covered with a plastic foil inpenetrable for beta$^-$-particles of ^{3}H. After the decay of ^{123}I (10 half-lives), the brain slices were exposed again to ^{3}H-sensitive imaging plates without plastic foil to obtain ^{3}H-Met distribution. In the case of the double-tracer comparison, ^{123}I-IMT versus ^{125}I-OMIMT a 10 times higher tracer dose was used for ^{123}I-IMT. Brain slices were exposed immediately after tracer injection and after decay of ^{123}I (10 half-lives) to obtain pure ^{125}I-OMIMT images.

Imaging plates were scanned by a phosphor imager (BAS 3000; Fuji Photofilm). The images were evaluated by regions of interest (ROIs) manually drawn around the whole tumor area and over a large area of normal brain tissue. Tracer uptake in the tumors was inhomogeneous, but none of the tumors showed larger areas of necrotic tissue with no tracer uptake. T/B ratios were determined by dividing the average photo-stimulated luminescence value per millimeter (*2*) of the tumor by that of the normal brain. Identical ROIs were used on the corresponding brain slices labeled with different tracers. In the ^{123}I-IMT versus ^{125}I-OMIMT comparison, the contamination of the tumor and the normal brain region by ^{125}I in the first exposure was calculated by measuring the photo-stimulated luminescence value per hour produced by ^{125}I in the second exposure. These values were subtracted from the data in the first exposure to obtain the true ^{123}I-IMT T/B ratio.

The tissue sections were stained with cresyl violet, which results in an intense coloration of Nissl-substance and nucleoli and is well suited to detect microscopically intracerebral tumor infiltration. The histological tumor extent was compared visually to that of the autoradiograms.

Statistical Analysis

Results are presented as mean ± s.d. Statistical methods used were the Student's t-test for group comparisons and Pearson's correlation coefficient. Probability values < 0.05 were considered to be significant.

RESULTS

Data of the T/B ratios found for the three different tracers are given in Table 1. The mean value of T/B ratios was 2.81 ± 0.78 for IMT (n = 14), 2.03 ± 0.57 for OMIMT (n = 17, $p < 0.01$ versus IMT) and 3.86 ± 1.12 for Met (n = 13, $p < 0.01$ versus IMT, $p < 0.001$ versus OMIMT). There was a significant correlation of the T/B ratios between all tracers (IMT versus Met: $r = 0.97$, n = 5, $p < 0.01$, Fig. 1A; OMIMT versus Met: $r = 0.94$, n = 8, $p < 0.001$, Fig. 1B; OMIMT versus IMT: $r = 0.95$, n = 9, $p < 0.001$, Fig. 1C). In relation to the T/B ratios of Met, those of IMT showed an increasing deviation from the line of unity in tumors with high uptake (Fig. 1A). This trend was even stronger for OMIMT (Fig. 1B).

Visual evaluation showed no difference in the pattern of intratumoral tracer distribution between the different tracers, and the extent of tumor labeling was identical to that of the histological tumor extent. An example of a comparison between autoradiograms of Met (left), IMT (middle) and histological staining using cresyl violet is given in Figure 2. T/B contrast of IMT is slightly lower than Met, but the tumor imaging of tumor extent and intratumoral tracer distribution is similar. Figure 3 compares autoradiograms of Met (left), OMIMT (middle) and

TABLE 1
Tumor-to-Brain Ratios of ^{3}H-Met, ^{123}I-IMT and $^{123/125}$I-OMIMT in Transplanted Rat Glioma Model

Rat no.	^{3}H-Met (tumor-to-brain)	^{123}I-IMT (tumor-to-brain)	$^{123/125}$I-OMIMT (tumor-to-brain)
1	3.65	3.02	—
2	3.98	3.09	—
3	3.03	2.3	—
4	4.77	3.46	—
5	5.46	3.80	—
6	3.84	—	2.10
7	4.55	—	2.30
8	1.89	—	1.40
9	4.69	—	2.40
10	3.6	—	1.60
11	4.67	—	2.30
12	1.67	—	1.23
13	4.42	—	2.00
14	—	3.01	2.61
15	—	2.32	1.68
16	—	3.29	2.52
17	—	1.70	1.57
18	—	2.01	1.53
19	—	3.84	3.35
20	—	1.40	1.26
21	—	2.56	2.10
22	—	3.59	2.50
Mean ± s.d.†	3.86 ± 1.12†	2.81 ± 0.78*	2.03 ± 0.57*

*$p < 0.01$ compared with $^{123/125}$I-OMIMT.
†$p < 0.001$ compared with $^{123/125}$I-OMIMT.
^{3}H-Met = [methyl-^{3}hydrogen]-L-methionine; ^{123}I-IMT = 3-[^{123}iodine]iodo-α-methyl-L-tyrosine; $^{123/125}$I-OMIMT = 3-[$^{123/125}$iodine]iodo-O-methyl-α-methyl-L-tyrosine.

histological staining (right). For OMIMT, the T/B contrast is considerably lower than of Met. Intratumoral tracer distribution is similar to that of Met, and the extent of the tumor labeling of both tracers is identical to that of cresyl violet staining.

DISCUSSION

In a previous study, we compared the results of PET with Met and SPECT with IMT in patients with cerebral gliomas (*15*). In that study, both methods yielded similar results concerning tumor size and intratumoral tracer distribution, but T/B ratios were slightly lower for IMT. It was confirmed by this study that imaging of cerebral gliomas with both tracers is identical with respect to tumor size and intratumoral tracer distribution. Since IMT, in contrast to Met, is not incorporated into protein, this result gives further support to the hypothesis that transport phenomena are of major importance for the increased uptake of large neutral amino acids in cerebral gliomas (*9,10,18*).

A frequently asked question is whether the increased uptake of amino acids in cerebral gliomas is caused by a disruption of the blood-brain barrier. It has been shown for Met, as well as for IMT, that uptake is also increased in low-grade gliomas without disruption of the blood-brain barrier (*2,3,7,11*) and that uptake in these tumors and in the normal brain can be competitively inhibited by intravenous infusion of other amino acids (*7,19*). It remains to be determined whether the increased uptake of amino acids in gliomas is caused by an increased number of amino acid carriers, by changes in substrate affinity of the carrier systems or by the appearance of additional carrier systems in glioma cells.

Although there was a good correlation in the T/B ratios between all tracers, the mean values of T/B ratios were significantly lower for IMT and OMIMT than for Met. Thus, the lower T/B ratios for SPECT with IMT as opposed to PET

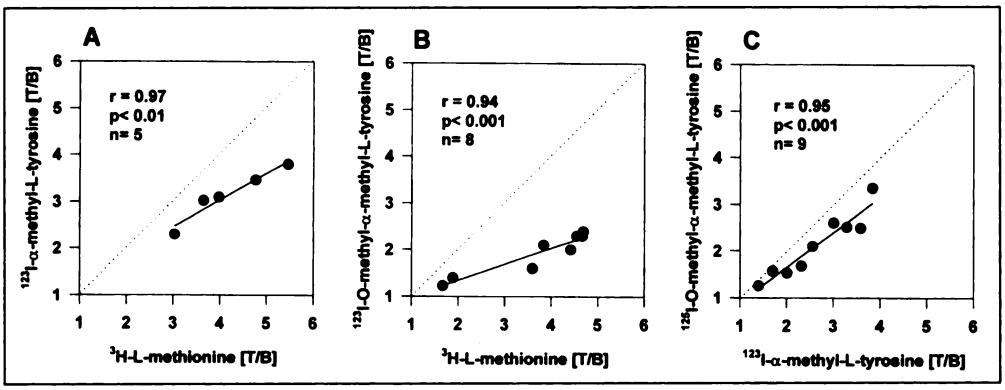

FIGURE 1. Comparison of tumor-to-brain (T/B) ratios for IMT, OMIMT and Met. There is significant correlation of T/B ratios among all tracers. (A) In relation to T/B ratios of Met, those of IMT showed increasing deviation from line of unity in tumors with high uptake. (B) This trend is even stronger for OMIMT. (C) The deviation from the line of unity is also obvious when comparing OMIMT to IMT.

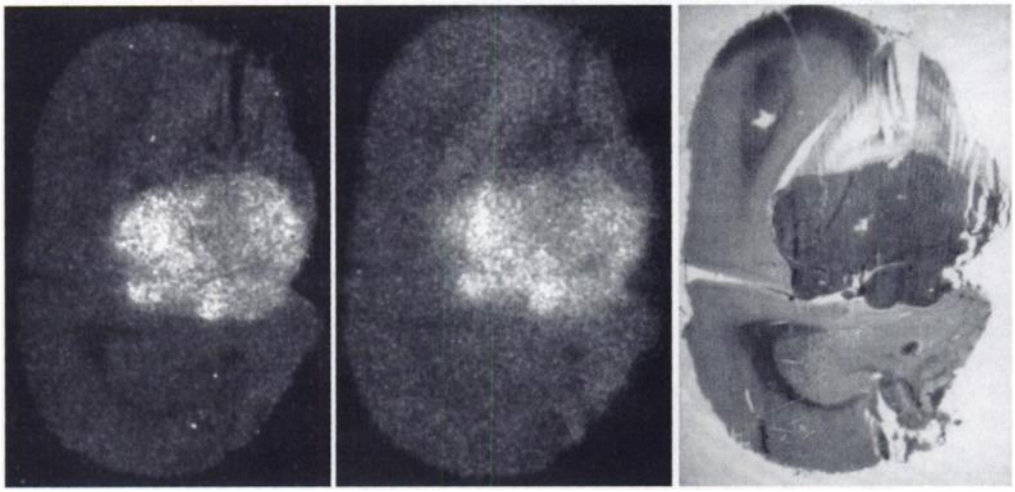

FIGURE 2. Comparison of autoradiograms of Met (left), IMT (middle) and histological staining using cresyl violet (right). Intratumoral tracer distribution is similar for IMT and Met. Tumor-to-brain contrast is slightly lower for IMT than for Met. Extent of tumor labeling is identical to that of cresyl violet staining.

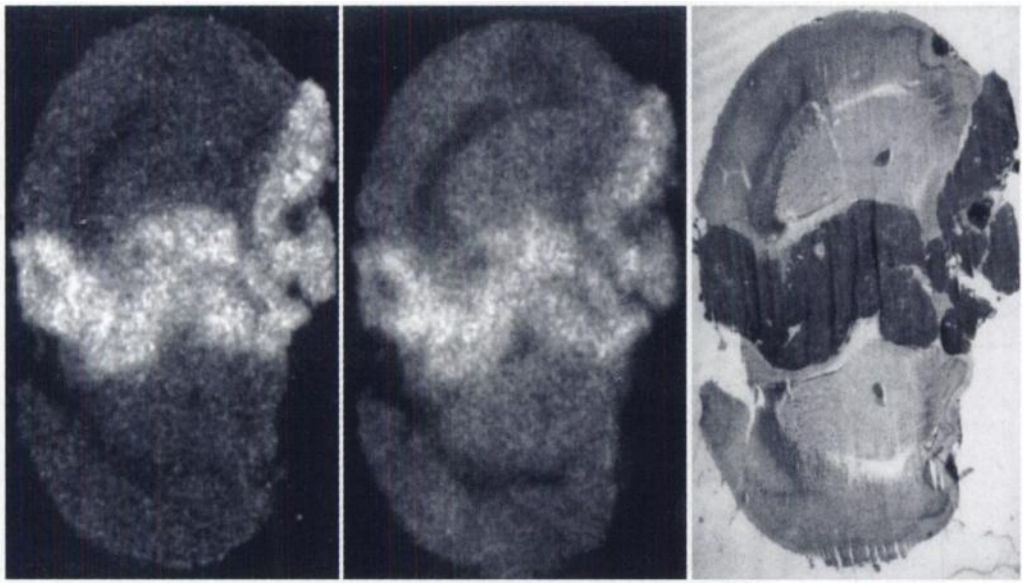

FIGURE 3. Comparison of autoradiograms of Met (left), OMIMT (middle) and histological staining using cresyl violet (right). Tumor-to-brain contrast is lower for OMIMT than for Met. Intratumoral tracer distribution is similar for IMT and Met. Extent of tumor labeling is identical to that of cresyl violet staining.

with Met, which were observed in the above-mentioned study (*15*), are not only explained by the technical differences between SPECT and PET but also by differences in the cerebral uptake of the tracers. The correlation analysis of T/B ratios between the Met and IMT autoradiograms showed that the T/B ratios deviated from the line of unity increasingly with higher T/B values. This effect was more strongly expressed for OMIMT than for IMT. It can be speculated that differences in the lipophilicity of Met, IMT and OMIMT may play a role in this phenomenon. Using the octanol-water partition coefficient, the lipophilicity of OMIMT compared to that of IMT was greater than a factor of two (*17*). The fivefold higher brain uptake of OMIMT compared to IMT observed in mice may be attributed to passive diffusion that flattens the T/B signal. The advantage of higher brain uptake of OMIMT is thus neutralized, and this amino acid seems to be unsuitable for clinical application. For IMT, the T/B ratios are also lower than for Met but still acceptable for clinical application. The clinical use of this amino acid has been demonstrated (*6,12–14*).

Study Limitations

The animal model used in this study is not an optimal model for the behavior of a human glioma. The glioma transplanted into a rat brain has a growth that more closely mimics that of a metastasis. There is, however, at present no better animal model. The shortcomings of the animal model have no impact on the comparisons of T/B ratios and intratumoral distribution of the different tracers.

CONCLUSION

This study confirms that tumor imaging with IMT is similar to that of Met, but T/B ratios of IMT were found to be significantly lower than for Met. For OMIMT, intratumoral tracer distribution and tumor size were similar to that of Met and IMT, but the T/B contrast was low, and this makes this amino acid less suitable for clinical application.

ACKNOWLEDGMENTS

The authors wish to thank Mr. M. Cremer for technical assistance in the animal experiments, Mrs. B. Palm, Mrs. E. Wabbals and Mrs. S. Bodé for technical assistance in radiosynthesis of 3-[^{123}I]iodo-α-methyl-L-tyrosine, Mr. H. Henneken for technical assistance in radiosynthesis of [$^{123/125}$I]iodo-O-methyl-α-methyl-L-tyrosine and Mrs. Koslowski and Mrs. D. Beaujean for secretarial assistance.

REFERENCES

1. Derlon JM, Boudet C, Bustany P, et al. Carbon-11-L-methionine uptake in gliomas. *Neurosurgery* 1989;25:720–728.
2. Ogawa T, Shishido F, Kanno I, et al. Cerebral glioma: evaluation with methionine PET. *Radiology* 1993;186:45–53.
3. Bergström M, Collins VP, Ehrin E, et al. Discrepancies in brain tumor extent as shown by CT and PET using ^{68}Ga-EDTA, ^{11}C-glucose and ^{11}C-methionine. *J Comput Assist Tomogr* 1983;7:1062–1066.
4. Mosskin M, Ericson K, Hindmarsh T, et al. PET compared with MRI and CT in supratentorial gliomas using multiple stereotactic biopsies as reference. *Acta Radiol* 1989;30:225–323.
5. Biersack HJ, Coenen HH, Stöcklin G, et al. Imaging of brain tumors with L-3-[^{123}I]iodo-α-methyl-tyrosine and SPECT. *J Nucl Med* 1989;30:110–112.
6. Langen K-J, Coenen HH, Roosen N, et al. SPECT studies of brain tumors with L-3-[^{123}I]iodo-α-methyl-tyrosine: comparison with PET, ^{124}IMT and first clinical results. *J Nucl Med* 1990;31:281–286.
7. Langen K-J, Roosen N, Coenen HH, et al. Brain and brain tumor uptake of L-3-[^{123}I]iodo-α-methyl-tyrosine: competition with natural L-amino acids. *J Nucl Med* 1991;32:1225–1228.
8. Kawai K, Fujibayashi Y, Saji H, et al. A strategy for the study of cerebral amino acid transport using iodine-123-labeled amino acid radiopharmaceutical: 3-iodo-α-methyl-L-tyrosine. *J Nucl Med* 1991;32:819–824.
9. Schober O, Meyer G-J, Stolke D, Hundeshagen H. Brain tumor imaging using C-11-labeled L-methionine and D-methionine. *J Nucl Med* 1985;26:98–99.
10. Wienhard K, Herholz K, Coenen HH, et al. Increased amino acid transport into brain tumors measured by PET of L-[2-^{18}F]fluoro-tyrosine. *J Nucl Med* 1991;32:1338–1346.
11. Coenen HH, Kling P, Stöcklin G. Cerebral metabolism of L-[2-^{18}F]fluoro-tyrosine: a new PET tracer of protein synthesis. *J Nucl Med* 1989;30:1367–1372.
12. Guth-Tougelidis B, Müller S, Mehdorn MM, et al. Anreicherung von DL-3-^{123}I-α-methyl-tyrosine in Hirntumor-Rezidiven. *Nuklearmedizin* 1995;34:71–75.
13. Kuwert T, Morgenroth C, Woesler B, et al. Uptake of iodine-123-α-methyl-tyrosine by gliomas and non-neoplastic brain lesions. *Eur J Nucl Med* 1996;23:1345–1353.
14. Schmidt D, Wunderlich G, Langen K-J, et al. Iodine-123-α-methyl-tyrosine (IMT) SPECT for evaluation of chemotherapy in cerebral gliomas [Abstract]. *J Nucl Med* 1996;37:354P.
15. Langen K-J, Ziemons K, Kiwit JCW, et al. Iodine-123-iodo-α-methyl-tyrosine SPECT and [^{11}C]-L-methionine uptake in cerebral gliomas: a comparative study using SPECT and PET. *J Nucl Med* 1997;38:517–522.
16. Krummeich C, Holschbach M, Stöcklin G. Direct n.c.a. electrophilic radioiodination of tyrosine analogues; their in vivo stability and brain uptake in mice. *Appl Radiat Isot* 1994;45:929–935.
17. Schmidt D, Langen K-J, Herzog H, et al. Whole-body kinetics and dosimetry of L-3-[^{123}I]iodo-α-methyl-tyrosine. *Eur J Nucl Med* 1997;24:1162–1166.
18. Ishiwata K, Kubota K, Murakami M, et al. Reevaluation of amino acid PET studies: can the protein synthesis rates in brain and tumor tissues be measured in vivo? *J Nucl Med* 1993;34:1936–1943.
19. Bergström M, Ericson K, Hagenfeldt L, et al. PET study of methionine accumulation in glioma and normal brain tissue: competition with branched chain amino acids. *J Comput Assist Tomogr* 1987;11:208–213.